Deuterium Labelling Hot Paper

How to cite: *Angew. Chem. Int. Ed.* **2022,** *61,* e202202423
International Edition: doi.org/10.1002/anie.202202423
German Edition: doi.org/10.1002/ange.202202423

# Manganese-Catalysed Deuterium Labelling of Anilines and Electron-Rich (Hetero)Arenes

*Florian Bourriquen, Nils Rockstroh, Stephan Bartling, Kathrin Junge,* and Matthias Beller**

**Abstract:** There is a constant need for deuterium-labelled products for multiple applications in life sciences and beyond. Here, a new class of heterogeneous catalysts is reported for practical deuterium incorporation in anilines, phenols, and heterocyclic substrates. The optimal material can be conveniently synthesised and allows for high deuterium incorporation using deuterium oxide as isotope source. This new catalyst has been fully characterised and successfully applied to the labelling of natural products as well as marketed drugs.

## Introduction

Constant growth in the use of deuterium-labelled compounds is observed in various scientific fields. Such compounds are of interest for instance as standards for mass spectrometry,[1] to prove reaction mechanisms,[2] to tune the properties of materials,[3,4] or to elucidate protein conformations.[5] However, they are mainly applied for the development of drugs in the pharmaceutical industry,[6–8] where labelling compounds is a prime technique for the investigation of metabolic pathways of a respective drug candidate. Interestingly, deuterium incorporation allows fine tuning of the pharmacokinetic properties of drug molecules, as the deuteration of specific positions might modify a drug's absorption, distribution, metabolism, and excretion properties. Furthermore, as C–D bond cleavage requires additional energy compared to C–H bonds, drugs containing labelled moieties can be more resistant towards metabolic degradation. As a result, a similar therapeutic effect might be achieved with a lower dosage. Consequently, in 2017, Austedo, the first deuterated drug on the market, was approved by the U.S. Food and Drug Administration for the treatment of chorea associated with Huntington's disease.[9]

[*] F. Bourriquen, Dr. N. Rockstroh, Dr. S. Bartling, Dr. K. Junge, Prof. Dr. M. Beller
Leibniz-Institut für Katalyse e.V.
Albert-Einstein-Straße 29a, 18059 Rostock (Germany)
E-mail: kathrin.junge@catalysis.de
matthias.beller@catalysis.de



Owing to the demand for labelled compounds, the development of novel, diverse methodologies for deuterium labelling has attracted considerable research interest.[10–12] Amongst the available methods, the most elegant is Hydrogen Isotope Exchange (HIE), where catalysts allow deuterium incorporation at specific positions. Consequently, HIE is of great importance for late-stage functionalisation of bioactive compounds.[13–19] In this respect, anilines are key building blocks in molecular chemistry, as reflected by their occurrence in 3 of the top 10 selling medications of 2019.[20] Owing to the significance of such compounds, a number of methodologies has been reported for the deuterium labelling of anilines (Scheme 1). For instance, deuterium incorporation is achieved at elevated temperatures by the use of strong bases[21] or acids, in particular hydrochloric and trifluoroacetic acids.[22,23] Recent studies showed such reactivity is equally feasible with perchloric acid at reduced temperatures.[24] Inherently, such approaches can be challenging in presence of acid-sensitive functional groups. Exploiting the concept of frustrated Lewis pairs, Werner and co-workers demonstrated the efficiency of the relatively

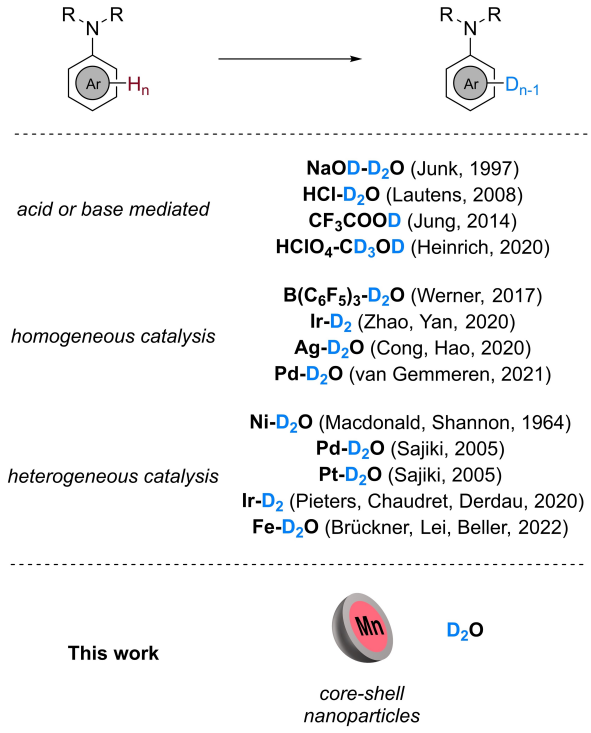


***Scheme 1.*** Selected approaches for the deuteration of aniline substrates (for respective references see text).

expensive tris(pentafluorophenyl)-borane as catalyst for H/D exchange at the *ortho*- and *para*-positions relative to the nitrogen using $D_2O$ as isotope source.[25] Additionally, molecularly defined complexes can efficiently promote H/D exchange in anilines such as the mesoionic carbene-iridium complex presented by Zhao, Yan and co-workers in 2020 for selective *ortho*-labelling.[26] However, despite the high deuterium content achieved, this methodology suffers by requiring a quantitative amount of base. The same year, a silver-catalysed methodology for HIE in electron-rich arenes was presented by Cong, Hao, and co-workers. Notably, this methodology is not limited to anilines, as nitrogen-containing heterocycles such as indoles and imidazoles could similarly undergo this transformation.[27] Recently, the van Gemmeren group introduced novel N,N-bidentate ligands embodying an *N*-acylsulfonamide moiety for the nondirected labelling of a broad scope of (hetero)arenes.[28] Here, one aniline substrate is presented with high deuterium incorporation at the *ortho*- and *para*-positions although concomitant labelling of the *meta*-position takes place to a lesser extent.

Due to the advantages regarding catalyst separation from reaction mixtures as well as potentially uncomplicated purification of the desired products, the use of heterogeneous catalysts became a topic of interest in HIE. In particular, in the presence of $D_2O$ and hydrogen, commercially available Pt/C and Pd/C are valuable tools for HIE at the aromatic and aliphatic positions, respectively,[29] and were successfully applied for the perdeuteration of anilines.[30,31] Besides, in line with work based on ruthenium nanoparticles,[32] Pieters, Chaudret, Derdau and co-workers presented air-stable NHC-stabilised iridium nanoparticles for HIE in anilines.[33] Employing deuterium gas as isotope source, *ortho*-deuteration is achieved with remarkable selectivity. Examples of the use of supported non-noble metals for aniline labelling are scarce. One of the rare instances applies Raney Nickel as described by Macdonald and Shannon already in 1964.[34]

Considering the increasing importance of labelled compounds, we envisioned the need for easy-to-operate and affordable methodologies for deuterium incorporation on multi-gram scale. In this respect, we recently disclosed the use of a simple pyrolysed iron catalyst for HIE.[35] Based on this work, we were interested in the development of new base-metal catalysed hydrogen/deuterium exchange reactions. Apart from iron, manganese appeared as an ideal candidate due to its availability, affordable price, and rich redox chemistry. While homogeneous manganese catalysts have been considerably investigated in recent years,[36,37] heterogeneous catalysts based solely on manganese were rarely studied, apart from electrocatalysis,[38–40] and there remain many opportunities in this area. In fact, to the best of our knowledge, no heterogeneous catalytic system for deuterium incorporation relying on manganese has been reported before. Noteworthily, here we present a practical methodology at comparably low catalyst loading and hydrogen pressure using $D_2O$ as the most affordable deuterium source available.

## Results and Discussion

At the start of this work, several iron and manganese salts were mixed with widely available biopolymers and subsequently pyrolysed at different temperatures. In this straightforward way it is possible to prepare a variety of the corresponding nanoparticles supported on carbon. All the materials were applied to the labelling of 4-methoxyaniline **1a** with $D_2O$ as model reaction. As depicted in Table S1, the pyrolysis process and support are crucial for the formation of active materials for isotopic labelling. More specifically, a temperature of 1000 °C and starch as carbon source gave the best results. Thus, nine starch-based materials consisting of different metals were synthesised and tested (Table S2). Remarkably, iron and manganese catalysts outperformed even noble metals such as ruthenium and palladium under our reaction conditions. Pleasingly, using Mn@Starch-1000 and employing deuterium oxide as isotope source, a deuterium incorporation of 94 % at the *ortho*-positions of **2a** is obtained using 20 mol % of metal under hydrogen pressure (Table 1, entry 1).[41] In the presence of organic co-solvents the deuterium incorporation decreased (Table 1, entries 2 and 3). On the contrary, water stable Lewis acids such as zinc, indium, or lanthanum triflates had no effect on the efficiency of this manganese-catalysed reaction. Surprisingly, an acidic media did not impede the catalyst activity while the labelling was lowered to 80 % in the presence of triethylamine and dropped to 34 % in the presence of a stronger base such as sodium hydroxide (Table 1, entries 5–7). Investigations of the gaseous atmosphere showed a similar deuterium incorporation under 20 bar of nitrogen instead of hydrogen. Lowering the catalyst loading to

***Table 1:*** Optimisation of reaction conditions.

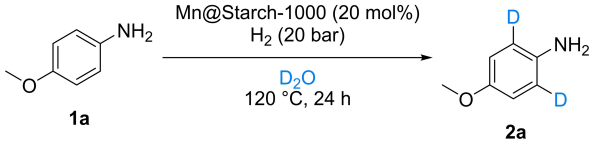


**1a** **2a**

| Entry[a] | Deviation from the standard conditions | Deuterium incorporation [%] |
|---|---|---|
| 1 | – | 94 |
| 2 | 100 °C instead of 120 °C | 30 |
| 3 | $^i$PrOH, THF or cyclohexane as co-solvents | 5–8 |
| 4 | Lewis acids as additives[b] | 93–94 |
| 5 | HCl as additive[b] | 93 |
| 6 | $NEt_3$ as additive[b] | 80 |
| 7 | NaOH as additive[b] | 34 |
| 8 | $N_2$ (20 bar) | 94 |
| 9 | $N_2$ (5 bar) | 81 |
| 10 | 10 mol % Mn, $H_2$ (5 bar) | 83 |
| **11** | **10 mol % Mn, $H_2$ (10 bar)** | **94** |
| 12 | no catalyst | < 5 |
| 13 | $Mn(OAc)_2{\cdot}4\,H_2O$ as catalyst[b] | 8 |
| 14 | Starch-1000 as catalyst[c] | < 5 |

[a] Reaction conditions: *p*-anisidine (0.25 mmol), Mn@Starch-1000 (58 mg, 20 mol % Mn), $H_2$ (20 bar), $D_2O$ (1.5 mL), 24 h, 120 °C. [b] 20 mol %. [c] 60 mg.

10 mol % still gave a deuteration yield of >80 % (Table 1, entries 10 and 11). Finally, control reactions showed poor labelling of the model substrate without the use of catalyst, or when manganese acetate or pyrolysed starch were used as catalysts (Table 1, entries 12–14).

Owing to the heterogeneous nature of the catalyst, its simple removal from the reaction mixture is achieved either by centrifugation or filtration, yielding deuterated *p*-anisidine **2a** without further purification. Recycling experiments of the recovered material were performed (see Supporting Information for details), revealing a reduced catalytic activity of the recycled material. To characterise the surface of our novel catalyst material and to understand the partial deactivation processes, initially X-ray Photoelectron Spectroscopy (XPS) measurements were applied.

Accordingly, the surface of the fresh catalyst consists mainly of C (96.2 at.%), O, and Mn as well as small amounts of Si, K, and P, probably residuals from the preparation process and/or support material, see Table S5 for quantification data and Figure S1 for survey spectra. The Mn concentration at the surface is rather low with about 0.2 at.%. The Mn 2p region with the Mn $2p_{3/2}$ peak at 641.5 eV is shown in Figure S2a. While the Mn 2p spectra of some oxidation states of Mn are rather similar,[42,43] the Mn 3s region has been mainly used to identify the present oxidation states and is shown in Figure S2c. Here, a peak distance of about 5.6 eV can be found, which indicates $Mn^{3+}$ as main oxidation state[43] for the fresh catalyst. Comparing the Mn 2p spectra of the fresh and recycled catalyst (Figure S2a and b), small structural changes can be noted. The satellite feature at 646 eV (an indication for MnO) is more pronounced in the recycled catalyst. Furthermore, the first fitting component at 639 eV is less intense in the recycled sample. Looking at the Mn 3 s region (Figure S2c and d), the two peaks for the fresh catalyst change in the recycled sample. Here, two broad features are observed indicating the coexistence of at least two different oxidation states like $Mn^{2+}$ and $Mn^{4+}$. It is important to mention that the surface concentration of Mn is very low, which makes the characterization challenging (especially for Mn 3s) even after long integration times. Next, Scanning Transmission Electron Microscopy (STEM) was applied to study the structural features of the fresh and recycled catalyst and to elucidate potential changes in the two samples. As can be seen in Figure 1, numerous $Mn/MnO_x$ core–shell particles are observed in fresh Mn@Starch-1000. The number of these particles is drastically reduced in the recycled Mn@Starch-1000 material, which in turn exhibits either Mn or $MnO_x$ particles, but in most cases no particles containing both Mn and $MnO_x$ (see Supporting Information). Generally, the Mn-containing particles are irregularly distributed over the support. The particle sizes of the Mn-containing particles cover a broad range in fresh Mn@Starch-1000, with the smallest being around 10 nm, the majority having sizes between 40 and 70 nm and the largest ones forming entities of up to 1.8 μm. These sizes remain relatively constant even after one reaction (see Supporting Information). In light of these two results, we presume that the decreased activity of the catalyst is related to these structural changes occurring during the course of the reaction.

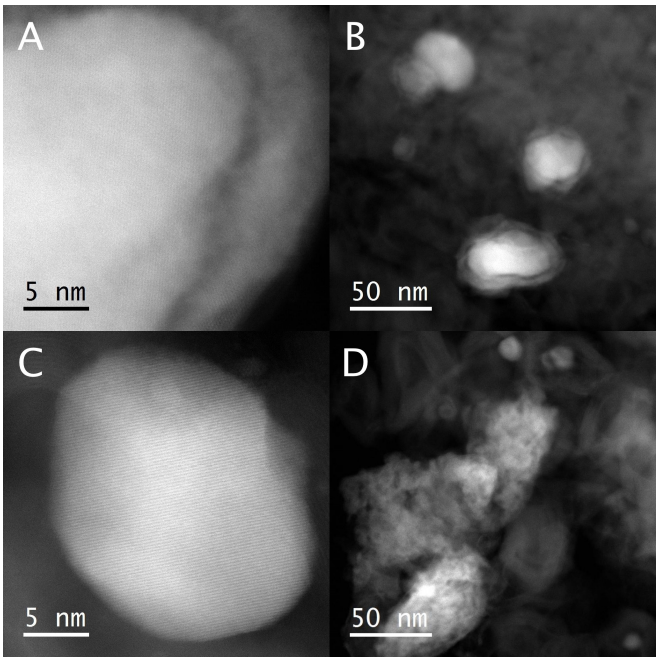


***Figure 1.*** HAADF-STEM images of A), B) Freshly prepared Mn@Starch-1000. C), D) Mn@Starch-1000 recovered after deuteration of *p*-anisidine at 120 °C, 10 bar $H_2$, 24 h in $D_2O$. While the fresh catalyst exhibits a considerable share of $Mn/MnO_x$ core–shell particles, there are predominantly either pure Mn (C) or pure $MnO_x$ particles present in the recycled catalyst.

With the optimised reaction conditions in hand (10 mol % Mn, 10 bar $H_2$, 120 °C, 24 h), we examined the scope of this novel catalyst system. The *ortho*- and *para*-positions of a variety of anilines were readily labelled with deuterium contents up to 98 % and high selectivity (Scheme 2). In particular, our model substrate *para*-anisidine **1a** can easily be converted in two steps to the common medication paracetamol.[44] Pleasingly, this catalyst material tolerates halogens (**2d**, **2e**, **2j**, **2k**) and the thioether functionality, as illustrated by the 82 % deuterium incorporation in 4-(methylthio)aniline **2b**. In addition, our procedure is not limited to primary amines, as secondary and tertiary amines such as 4-phenylmorpholine **1h** were smoothly deuterated. Moreover, the 4-position of 3,5-di-*tert*-butylaniline **2i** was successfully deuterated, highlighting the possibility of labelling sterically demanding substrates. The high specificity of this process towards labelling electron-rich aromatic rings is emphasised when *N*-benzylaniline **1m** was tested as substrate. Indeed, the benzyl ring was unaffected, and exclusively the aniline ring of **2m** was labelled with excellent deuterium incorporation (98 %). A comparable result is observed with 9*H*-fluoren-2-amine **1l**. Interestingly, in this case labelling of the activated C9 position concomitantly takes place. Anilines containing allyl as well as hydroethyl moieties are also efficiently converted to their deuterated counterparts (**2n**, **2o**). Finally, anilines containing electron-withdrawing substituents were subjected

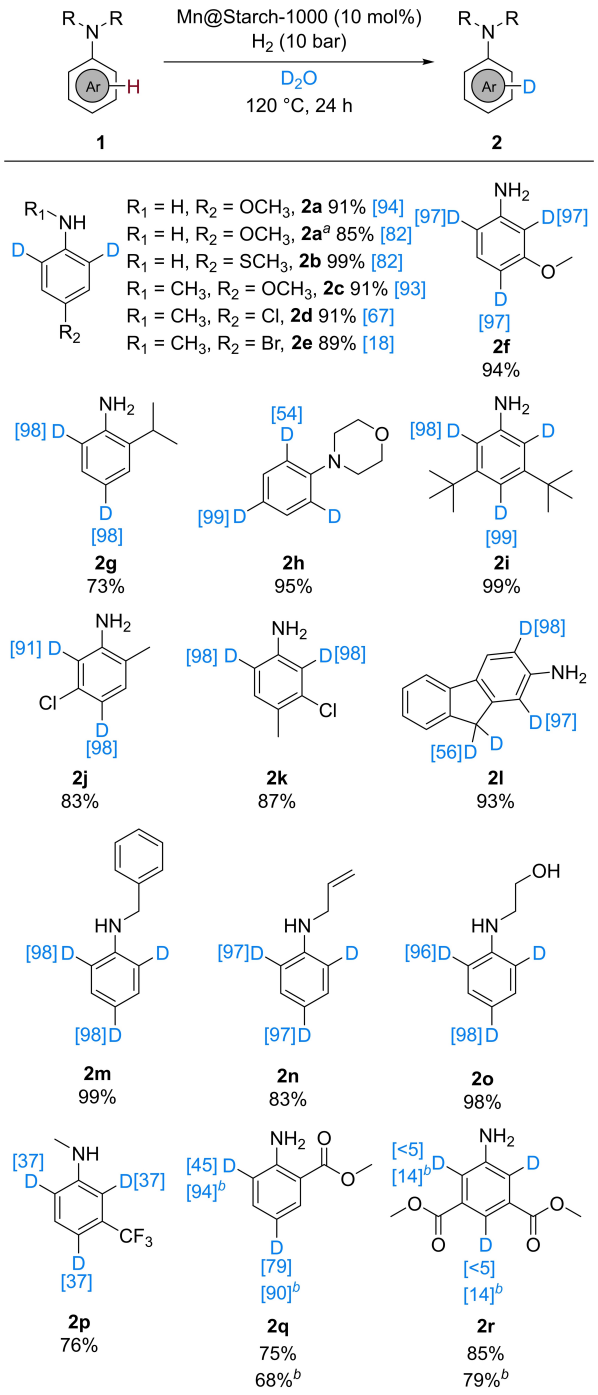


***Scheme 2.*** Scope of anilines. Substrate (0.5 mmol), Mn@Starch-1000 (58 mg, 10 mol% Mn), $H_2$ (10 bar), $D_2O$ (1.5 mL), 120 °C, 24 h. Isolated yields. The blue numbers between brackets represent the deuterium incorporation. [a] 1 g scale. [b] 140 °C.

to our labelling procedure. Unsurprisingly, the deuterium content is reduced, as it was already observed in chloro- and bromo-containing substituents (**2d**, **2e**). Nevertheless, even in the presence of a trifluoromethyl group (**2p**) deuterium incorporation of 37% is detected. Moderate to high deuterium contents (45% and 79% at the *ortho*- and *para*-positions, relative to the amine, respectively) are obtained with methyl 2-aminobenzoate (**2q**). In this case, an increased reaction temperature provides a 90% deuterium incorporation at both positions. However, for electron-poor arenes such as **1r**, bearing two methyl ester substituents, a 140 °C reaction temperature does not lead to an elevated deuterium incorporation.

Next, we were interested in the applicability of this catalytic system for the labelling of nitrogen-containing heterocycles (Scheme 3). Under standard reaction conditions, complete deuterium incorporation occurred at the 2-position of imidazole (**2s**, **2t**) and benzimidazole (**2u**) moieties, while the other hydrogen atoms were left untouched. On the other hand, the labelling of indoles was significantly conditioned by ring substituents. For example, when 1-methyl-2-phenyl-1*H*-indole **1v** was subjected to our procedure, deuterium incorporation was exclusively de-

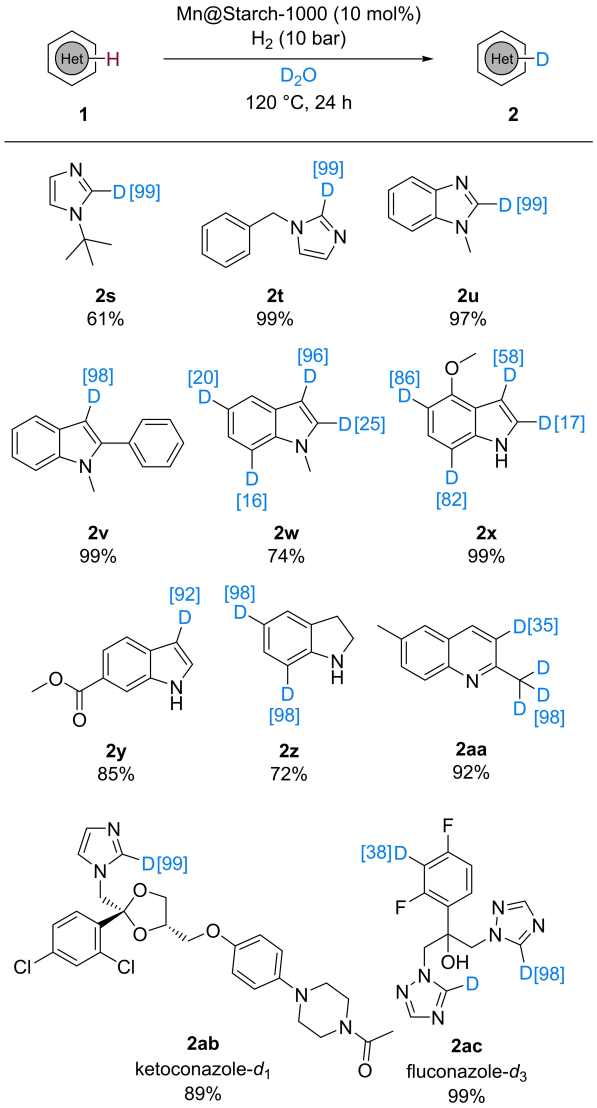


***Scheme 3.*** Scope of N-containing heterocycles. Substrate (0.5 mmol), Mn@Starch-1000 (58 mg, 10 mol% Mn), $H_2$ (10 bar), $D_2O$ (1.5 mL), 120 °C, 24 h. Isolated yields. The blue numbers between brackets represent the deuterium incorporation.

tected at the 3-position. However, 1-methyl-1*H*-indole **1w** also showed deuterium incorporation on the benzene ring. Naturally, an electron-donating substituent such as the methoxy group increases the deuterium incorporation (**2x**), whereas the methyl ester moiety present in **2y** limited the deuterium content. Indoline **1z** reacted smoothly and provided the deuterated analogue **2z** with 98% deuterium incorporation. The protons from the activated methyl group in 2,6-dimethylquinoline (**1aa**) smoothly underwent H/D exchange, however, the exchange took place to a limited extent with the aromatic protons, with merely 35% deuterium detected at the 3-position of the quinoline scaffold.

The introduction of deuterium atoms in drug candidates and marketed drugs is highly desirable, see above. To demonstrate the potential of the presented methodology, the 5-position of the triazole ring of fluconazole, a commercial antifungal medication, was efficiently labelled. Moreover, the 3-position of the phenyl ring neighbouring both fluorine atoms was concomitantly labelled, providing fluconazole-$d_3$ (**2ac**) in quantitative yield. Likewise, the imidazole ring of ketoconazole showed a comparable reactivity to more simple model substrates and afforded ketoconazole-$d_1$ (**2ab**) with a quantitative deuterium incorporation.[45]

Furthermore, a variety of phenol substrates were labelled using our Mn@Starch-1000 catalyst (Scheme 4). In general, these substrates exhibit a poorer reactivity compared to anilines. Nevertheless, for most applied substrates good deuterium incorporation was observed, albeit at higher temperature. Electron-rich aminophenols (**2ad**, **2ae**) and a catechol derivative **2af** provided high D content at 120 °C. Mixed outcomes were obtained with dimethylphenols: while 2,5-dimethylphenol (**1ag**) is smoothly labelled under our standard reaction conditions, higher temperature was necessary to achieve a similar isotope incorporation in 2,3-dimethylphenol (**1ah**). Phenol **1ai** yielded a medium deuterium content. Deuterated analogues of monoterpenoids carvacrol and thymol (**2aj**, **2ak**) are produced using our manganese-catalysed methodology, underlining its applicability to natural products. Finally, electron-rich 1,3,5-trimethoxybenzene reacted efficiently and provided **2al** with 93% D.

To gain information on the reaction mechanism, we performed our model reaction in the presence of TEMPO as a radical scavenger (Scheme 5). In this case, the deuterium incorporation was drastically lowered to only 12%, strongly suggesting a radical mechanism. Additionally, performing the reaction using $D_2$ gas in water showed no deuterium incorporation, highlighting the importance of the $D_2O/H_2$ combination for efficient labelling. Besides, using $D_2$ as reductant instead of $H_2$ lowered the labelling of *p*-anisidine from 94% to 85%, providing a secondary kinetic isotope effect of 1.1. Due to the similarity in the catalysts' structures and reactivity, we propose a mechanism similar to the one discussed in our previous iron-mediated labelling methodology is likely to be taking place: homolytic $D_2O$ cleavage by Mn@Starch-1000 generates D* and DO* radicals. A hydrogen atom from the substrate is abstracted by DO* providing

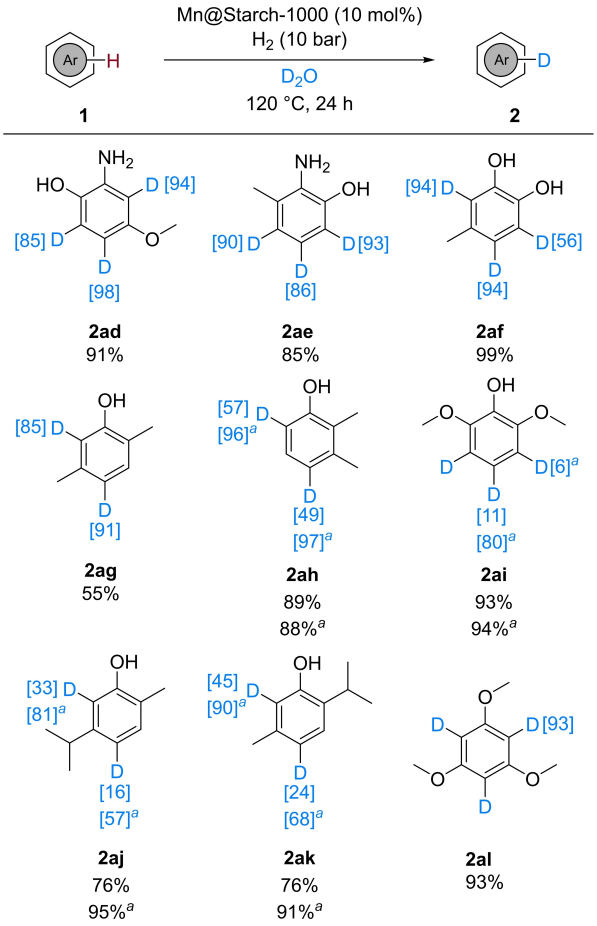


***Scheme 4.*** Scope of phenols and electron-rich arenes. Substrate (0.5 mmol), Mn@Starch-1000 (58 mg, 10 mol% Mn), $H_2$ (10 bar), $D_2O$ (1.5 mL), 120 °C, 24 h. Isolated yields. The blue numbers between brackets represent the deuterium incorporation. [a] 140 °C.

HDO and a phenyl radical which subsequently reacts with D* yielding the deuterated product.[35] Interestingly, both de-deuteration of 2,4,6-trideuteroaniline and deuteration of 3,5-dideuteroaniline showed a positive kinetic isotope effect, the latter suggesting a different coordination of the aniline substrate on the catalyst's surface.

## Conclusion

In conclusion, we report here the first example of a heterogeneous manganese catalyst, Mn@Starch-1000, for hydrogen isotope exchange reactions. The key to success for the deuterium incorporation is the formation of $Mn/MnO_x$ core–shell particles supported on pyrolysed carbon. Notably, the concentration of manganese on the surface is rather low, demonstrating the high activity of these active centres. The presented practical methodology tolerates a range of functional groups and was successfully implemented for the labelling of electron-rich arenes and heteroarenes. Importantly, this strategy profits from the use of deuterium oxide as an easy-to-handle isotope source and is a competitive

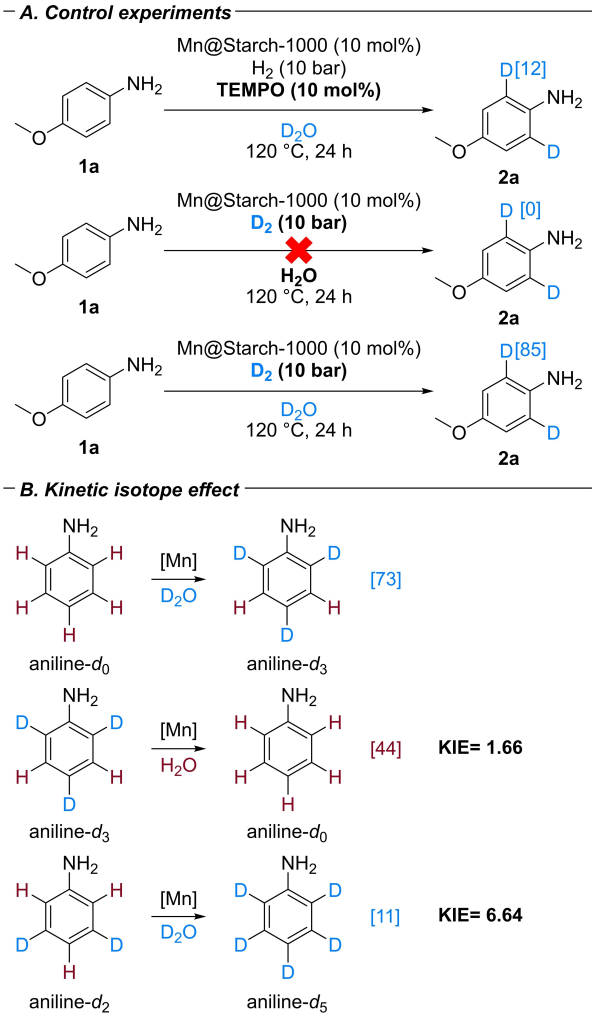


***Scheme 5.*** Control experiments – Kinetic isotope effect. Aniline substrate (0.5 mmol), Mn@Starch-1000 (30 mg, 5 mol% Mn), $H_2$ (10 bar), $H_2O$ or $D_2O$ (1.5 mL), 120 °C, 5 h.

alternative to more classical procedures relying on noble metals.

## Acknowledgements

We thank the analytical staff of the LIKAT for their excellent service. Sara Kopf and Dr. Wu Li are thanked for valuable discussions with respect to deuterium incorporation. We thank Dr. Wolfgang Baumann for performing deuterium NMR experiments. We thank Dr. Peter McNeice for assistance during preparation of the manuscript. This project has received funding from the European Union's Horizon 2020 research and innovation program under grant agreement No 862179. We also acknowledge the European Research Council (EU project 670986-NoNaCat) and the State of Mecklenburg-Vorpommern for financial and general support. Open Access funding enabled and organized by Projekt DEAL.

## Conflict of Interest

The authors declare no conflict of interest.

## Data Availability Statement

The data that support the findings of this study are available in the Supporting Information of this article.

**Keywords:** Deuterium · Heterogeneous Catalysis · Hydrogen Isotope Exchange · Manganese · Starch

[1] J. Atzrodt, V. Derdau, *J. Labelled Compd. Radiopharm.* **2010**, *53*, 674–685.
[2] E. M. Simmons, J. F. Hartwig, *Angew. Chem. Int. Ed.* **2012**, *51*, 3066–3072; *Angew. Chem.* **2012**, *124*, 3120–3126.
[3] M. Shao, J. Keum, J. Chen, Y. He, W. Chen, J. F. Browning, J. Jakowski, B. G. Sumpter, I. N. Ivanov, Y.-Z. Ma, C. M. Rouleau, S. C. Smith, D. B. Geohegan, K. Hong, K. Xiao, *Nat. Commun.* **2014**, *5*, 3180.
[4] J. B. Grimm, L. Xie, J. C. Casler, R. Patel, A. N. Tkachuk, N. Falco, H. Choi, J. Lippincott-Schwartz, T. A. Brown, B. S. Glick, Z. Liu, L. D. Lavis, *JACS Au* **2021**, *1*, 690–696.
[5] L. Konermann, J. Pan, Y.-H. Liu, *Chem. Soc. Rev.* **2011**, *40*, 1224–1234.
[6] T. G. Gant, *J. Med. Chem.* **2014**, *57*, 3595–3611.
[7] J. Atzrodt, V. Derdau, W. J. Kerr, M. Reid, *Angew. Chem. Int. Ed.* **2018**, *57*, 1758–1784; *Angew. Chem.* **2018**, *130*, 1774–1802.
[8] T. Pirali, M. Serafini, S. Cargnin, A. A. Genazzani, *J. Med. Chem.* **2019**, *62*, 5276–5297.
[9] C. Schmidt, *Nat. Biotechnol.* **2017**, *35*, 493–494.
[10] J. Atzrodt, V. Derdau, T. Fey, J. Zimmermann, *Angew. Chem. Int. Ed.* **2007**, *46*, 7744–7765; *Angew. Chem.* **2007**, *119*, 7890–7911.
[11] J. Atzrodt, V. Derdau, W. J. Kerr, M. Reid, *Angew. Chem. Int. Ed.* **2018**, *57*, 3022–3047; *Angew. Chem.* **2018**, *130*, 3074–3101.
[12] S. Kopf, F. Bourriquen, W. Li, H. Neumann, K. Junge, M. Beller, *Chem. Rev.* **2022**, *122*, 6634–6718.
[13] C. Zarate, H. Yang, M. J. Bezdek, D. Hesk, P. J. Chirik, *J. Am. Chem. Soc.* **2019**, *141*, 5034–5044.
[14] A. Palazzolo, S. Feuillastre, V. Pfeifer, S. Garcia-Argote, D. Bouzouita, S. Tricard, C. Chollet, E. Marcon, D.-A. Buisson, S. Cholet, F. Fenaille, G. Lippens, B. Chaudret, G. Pieters, *Angew. Chem. Int. Ed.* **2019**, *58*, 4891–4895; *Angew. Chem.* **2019**, *131*, 4945–4949.
[15] V. Müller, R. Weck, V. Derdau, L. Ackermann, *ChemCatChem* **2020**, *12*, 100–104.
[16] Q.-K. Kang, H. Shi, *Synlett* **2021**, *32*, A–J.
[17] V. Pfeifer, T. Zeltner, C. Fackler, A. Kraemer, J. Thoma, A. Zeller, R. Kiesling, *Angew. Chem. Int. Ed.* **2021**, *60*, 26671–26676; *Angew. Chem.* **2021**, *133*, 26875–26880.
[18] A. Tlahuext-Aca, J. F. Hartwig, *ACS Catal.* **2021**, *11*, 1119–1127.
[19] A. Uttry, S. Mal, M. van Gemmeren, *J. Am. Chem. Soc.* **2021**, *143*, 10895–10901.
[20] V. A. Schmidt, *Nature* **2020**, *584*, 46–47.
[21] T. Junk, W. J. Catallo, L. D. Civils, *J. Labelled Compd. Radiopharm.* **1997**, *39*, 625–630.
[22] A. Martins, M. Lautens, *Org. Lett.* **2008**, *10*, 4351–4353.
[23] R. Giles, A. Lee, E. Jung, A. Kang, K. W. Jung, *Tetrahedron Lett.* **2015**, *56*, 747–749.
[24] O. Fischer, A. Hubert, M. R. Heinrich, *J. Org. Chem.* **2020**, *85*, 11856–11866.

[25] W. Li, M.-M. Wang, Y. Hu, T. Werner, *Org. Lett.* **2017**, *19*, 5768–5771.
[26] W. Liu, L. Cao, Z. Zhang, G. Zhang, S. Huang, L. Huang, P. Zhao, X. Yan, *Org. Lett.* **2020**, *22*, 2210–2214.
[27] B. Dong, X. Cong, N. Hao, *RSC Adv.* **2020**, *10*, 25475–25479.
[28] M. Farizyan, A. Mondal, S. Mal, F. Deufel, M. van Gemmeren, *J. Am. Chem. Soc.* **2021**, *143*, 16370–16376.
[29] H. Sajiki, N. Ito, H. Esaki, T. Maesawa, T. Maegawa, K. Hirota, *Tetrahedron Lett.* **2005**, *46*, 6995–6998.
[30] I. Nobuhiro, E. Hiroyoshi, M. Tsuneaki, I. Eikoh, M. Tomohiro, S. Hironao, *Bull. Chem. Soc. Jpn.* **2008**, *81*, 278–286.
[31] N. Ito, T. Watahiki, T. Maesawa, T. Maegawa, H. Sajiki, *Synthesis* **2008**, *2008*, 1467–1478.
[32] G. Pieters, C. Taglang, E. Bonnefille, T. Gutmann, C. Puente, J.-C. Berthet, C. Dugave, B. Chaudret, B. Rousseau, *Angew. Chem. Int. Ed.* **2014**, *53*, 230–234; *Angew. Chem.* **2014**, *126*, 234–238.
[33] M. Valero, D. Bouzouita, A. Palazzolo, J. Atzrodt, C. Dugave, S. Tricard, S. Feuillastre, G. Pieters, B. Chaudret, V. Derdau, *Angew. Chem. Int. Ed.* **2020**, *59*, 3517–3522; *Angew. Chem.* **2020**, *132*, 3545–3550.
[34] C. G. Macdonald, J. S. Shannon, *Tetrahedron Lett.* **1964**, *5*, 3351–3354.
[35] W. Li, J. Rabeah, F. Bourriquen, D. Yang, C. Kreyenschulte, N. Rockstroh, H. Lund, S. Bartling, A.-E. Surkus, K. Junge, A. Brückner, A. Lei, M. Beller, *Nat. Chem.* **2022**, *14*, 334–341.
[36] J. R. Carney, B. R. Dillon, S. P. Thomas, *Eur. J. Org. Chem.* **2016**, 3912–3929.
[37] Y. Wang, M. Wang, Y. Li, Q. Liu, *Chem* **2021**, *7*, 1180–1223.
[38] J.-S. Lee, G. S. Park, H. I. Lee, S. T. Kim, R. Cao, M. Liu, J. Cho, *Nano Lett.* **2011**, *11*, 5362–5366.
[39] C. Walter, P. W. Menezes, S. Orthmann, J. Schuch, P. Connor, B. Kaiser, M. Lerch, M. Driess, *Angew. Chem. Int. Ed.* **2018**, *57*, 698–702; *Angew. Chem.* **2018**, *130*, 706–710.
[40] B. Zhang, J. Zhang, J. Shi, D. Tan, L. Liu, F. Zhang, C. Lu, Z. Su, X. Tan, X. Cheng, B. Han, L. Zheng, J. Zhang, *Nat. Commun.* **2019**, *10*, 2980.
[41] These initial screening conditions correspond to the optimised reaction conditions from reference [35].
[42] M. C. Biesinger, B. P. Payne, A. P. Grosvenor, L. W. M. Lau, A. R. Gerson, R. S. C. Smart, *Appl. Surf. Sci.* **2011**, *257*, 2717–2730.
[43] E. S. Ilton, J. E. Post, P. J. Heaney, F. T. Ling, S. N. Kerisit, *Appl. Surf. Sci.* **2016**, *366*, 475–485.
[44] S. Singh, K. K. Roy, S. R. Khan, V. K. Kashyap, A. Sharma, S. Jaiswal, S. K. Sharma, M. Y. Krishnan, V. Chaturvedi, J. Lal, S. Sinha, A. Dasgupta, R. Srivastava, A. K. Saxena, *Bioorg. Med. Chem.* **2015**, *23*, 742–752.
[45] Absence of deuterium incorporation on the aniline scaffold can be attributed to the interaction of the amide moiety with the catalyst surface; thus, impeding coordination of the aniline.

Manuscript received: February 14, 2022
Accepted manuscript online: April 29, 2022
Version of record online: May 12, 2022